doi.org/10.15407/tpwj2016.08.04

FORMATION OF WELD METAL STRUCTURE IN ELECTRON BEAM WELDING OF SINGLE CRYSTALS OF HIGH-TEMPERATURE NICKEL ALLOYS

K.A. YUSHCHENKO[1], B.A. ZADERY[1], I.S. GAKH[1] and **O.P. KARASEVSKAYA[2]**
[1]E.O. Paton Electric Welding Institute, NASU
11 Kazimir Malevich Str., 03680, Kiev, Ukraine. E-mail: office@paton.kiev.ua
[2]G.V. Kurdyumov Institute for Metal Physics, NASU
35 Acad. Vernadsky Ave., 03680, Kiev, Ukraine. E-mail: Karas@imp.kiev.ua

Investigations of the features of temperature-rate parameters of weld pool metal solidification in EBW of single crystals of high-temperature nickel alloys were the basis for establishing the peculiarities of their influence on ensuring the single-crystal structure. Investigations were performed on single-crystal samples of commercial high-temperature nickel alloy JS26 with application of methods of thermometry of liquid pool melt during weld metal solidification at cooling. The structures were studied with application of methods of microprobe analysis, optical and electron metallography and XRD. A computational-experimental procedure for determination of temperature-rate parameters of weld metal solidification is proposed, the nature of their variation across weld pool solidification front is shown, and the interrelation with the welding modes is established. The range of parameter values was determined, in which grains with random crystallographic orientation form in the weld. The possibility of controlling the structural perfection of weld metal through optimization of temperature-rate parameters of solidification is shown. 23 Ref., 4 Tables, 10 Figures.

Keywords: *single crystal, high-temperature nickel alloy, temperature-rate conditions, temperature gradient, crystallographic orientation, weld, orientation of predominant crystal growth, direction of maximum temperature gradient, randomly oriented grains*

The degree of structure perfection is one of the main factors, determining service characteristics of single crystals of such high-temperature nickel alloys (HTNA) as heat resistance, ductility, fatigue resistance, etc. [1–10]. Quality of single-crystal structure is determined by the following crystallographic and structural features: crystallographic orientation and degree of disorientation of structural elements, parameters of structural components, and absence of grains differing from base metal by their crystallographic orientation.

In work [11–14] it is shown that the following features are the indications of structure perfection in welded joints of HTNA single crystals:

- structural alignment of weld metal, HAZ and base metal (with not more than 5° deviation);
- absence of randomly oriented grains in weld metal, which are considered to be the main defect of single crystals.

Producing such welds (Figures 1 and 2) is possible, when the following conditions are fulfilled:

- fusion surface and welding direction should not deviate from crystallographic orientation (001) by more than 3°;
- deviation of the direction of maximum temperature gradient from crystallographic orientation of predominant growth <100> on weld pool solidification front should be not more than 15°.

Technological support for fulfilling the first condition is provided by crystallographically oriented preparation of welded joint elements; and for the second condition it is ensured through control of weld pool shape at the stage of its solidification. The most favourable initial orientational conditions for producing welds with perfect single-crystal structure are provided at coincidence of butt edges with crystallographic plane {001} (see Figure 1) — symmetrical structure of the joint. In practice such initial conditions cannot always be ensured, for instance, in re-

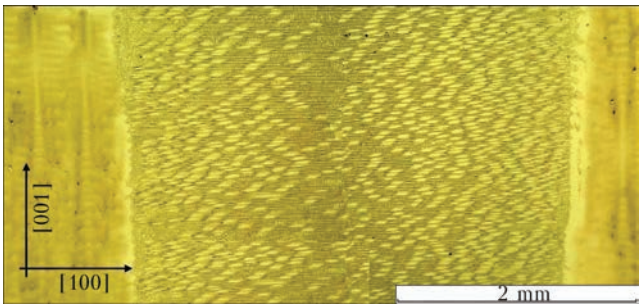

Figure 1. Microstructure of single-crystal welded joint of JS32 alloy produced when controlling orientational parameters of weld metal solidification

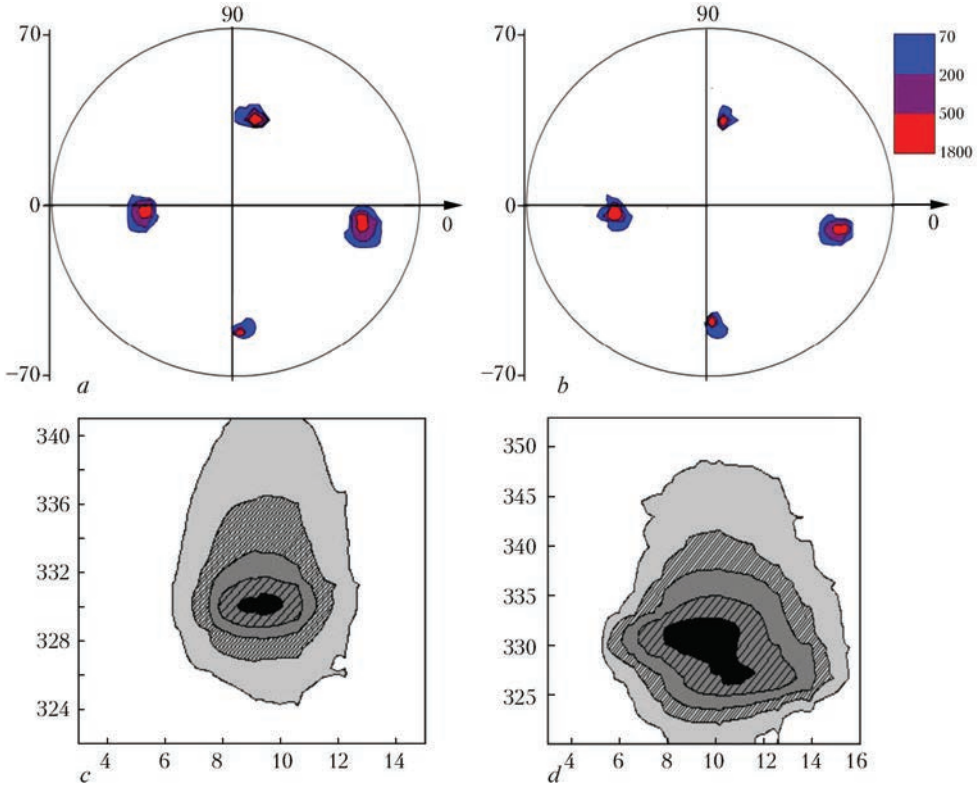

Figure 2. Pole figures {220} (*a*, *b*) and $I\mathbf{q}_{\perp}$ distribution of (200) reflection (*c*, *d*) in different zones of welded joint produced when controlling orientational parameters of weld metal solidification: *a*, *b* — BM, *c*, *d* — weld metal (numerical values along the axes are given in degrees)

pair operations, or in welding structures of a complex shape, as well as at performance of multipass welds.

In the joints with fusion surface initial orientation close to {111}, up to 80 % of randomly oriented grains can form in the weld metal. At unfavourable weld pool geometry in joints with symmetrical crystallographic structure, grain percentage can be equal to 4–10 %. Therefore, producing welds meeting the above quality criteria on single crystals of asymmetrical crystallographic orientation is a problem. Its solution was addressed, using the known postulate of the theory of crystallization, namely, the quality of single crystal growth is determined chiefly by crystallography of initial blank (seed) and temperature-rate conditions of solidification. It is known [6, 8–10] that optimum parameters of structure in casting HTNA single crystal growth are achieved, when temperature-rate and orientational conditions of directional solidification are provided. The main of them are evaluated by magnitude and direction of maximum temperature gradient **G** across the solidification front, solidification rate **R**, their ratio **G/R**, and crystallographic orientation of the starting seed.

When growing single crystals, these parameters determine solidification kinetics across the solidification front and have a dominant influence on formation of structural and crystallographic parameters of single-crystal casting (degree of perfection of single-crystal structure, dendritic structure dispersion, morphology and size of secondary phases). **G/R** ratio determines the type and perfection of the structure and susceptibility to formation of randomly-oriented grains (ROG), and **GR** product determines the dispersity of structural components. When growing HTNA single crystals, optimum values of the above factors have been established and are achieved due to design features of equipment and technological parameters of liquid-metal cooler, heater and the process proper.

In welding such optimization is possible due to selection of distribution of heat source power, as well as rate and schematic of welded joint formation process. However, while the regularities of technological parameters influence on the extent of the change of the above temperature-rate conditions of formation have been well studied when growing single crystals [6, 8–10], such data for welding are quite limited in published sources, particularly, for substantiation of recommendations on controlling weld metal structure formation. Such a situation is attributable, mainly, to procedural difficulties, related to transient and non-equilibrium nature of the process of pool solidification, small volume and short time of its existence, high level and gradient of temperatures, variable rate and direction of crystallite growth across the weld pool front. The scarce publications give only the integral values of temperature gradient level and average

solidification rate [15–18]. These results were obtained predominantly by computational method, and the connection of thermophysical factors (**G**, **R**) of solidification with crystallographic and structural parameters of weld metal and technological conditions of joint formation is not revealed.

The objective of this work was studying the influence of temperature-rate and orientational conditions of solidification of weld pool metal on perfection of single-crystal structure, susceptibility to ROG formation, weld metal structure parameters, determination of the range of temperature-rate conditions of ROG formation in EBW of commercial HTNA with single-crystal structure.

In order to study the kinetics of temperature-rate parameters of solidification process at formation of weld metal structure, a special procedure was developed with application of local thermometry of liquid pool melt and weld metal in EBW. Proposed sample geometry and experimental schematic (Figures 3 and 4) allow evaluation of temperature parameters in a particular selected region of weld pool, in order to establish the interrelation with the characteristics of weld metal structure for this region.

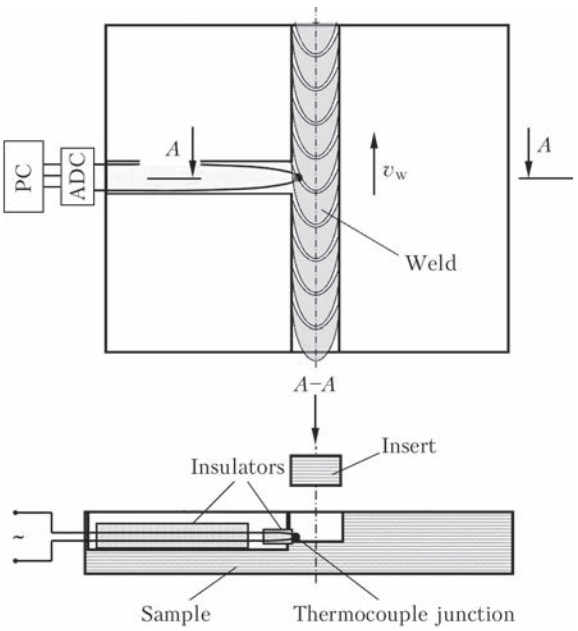

Figure 3. Schematic of thermometry of the process of weld metal solidification and sample geometry

Investigations were conducted on samples of commercial JS26 and JS32 HTNA with single-crystal structure (Table 1), 2.5 mm thick. Welding experiments were performed in the range of speeds of

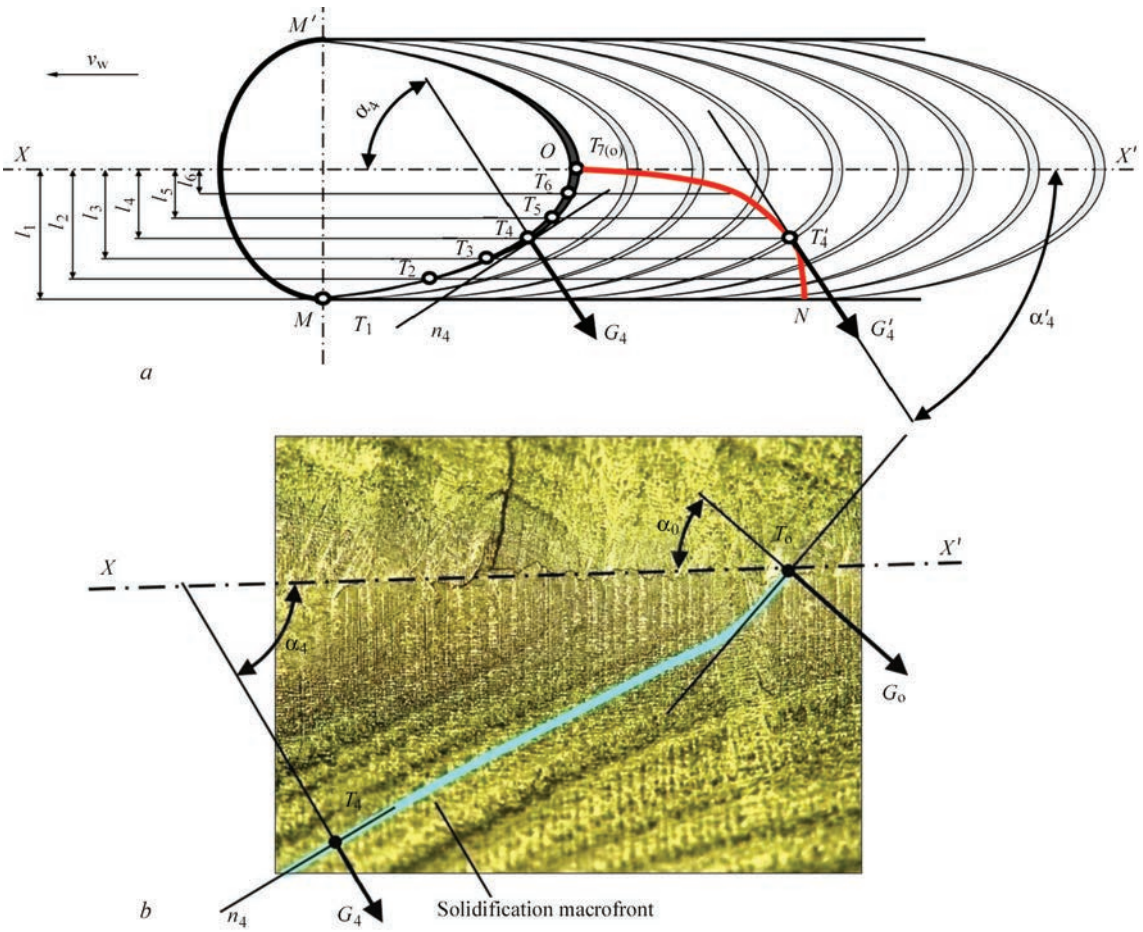

Figure 4. Schematic of weld pool (*a*) for evaluation of angle α of deviation of the direction of maxim temperature gradient **G** across weld pool solidification macrofront *MOM′* (*b*): *ON* — curve of the change of maximum temperature gradient over solidification macrofront across weld section; *XX″* — weld axis

Table 1. Composition of the studied HTNA [10]

Alloy	Average values, wt.%											
	C	Cr	Co	W	Mo	Ti	Al	Nb	V	Re	Ta	B
JS26	0.15	5.0	9.0	5–15	0.5–5.0	0.2–4.0	4.5–8.0	1.6	1.0	–	–	0.01–0.30
JS32	0.15	5.0	9.3	2–10	0.5–5.0	–	4.5–8.0	1.5–5.0	–	4.0	4.0	0.01–0.30

12–90 m/h. Other parameter values were selected proceeding from the conditions of complete penetration and formation of welds with parallel fusion surfaces.

W-Re_s–W-Re_{20} thermocouples of 0.2 mm diameter were used. Thermocouple junction of up to 0.8 mm diameter, made by EBW, was covered by powder of aluminium oxide with a binder. This provided a thin dielectric layer, preventing signal shunting, and not affecting measurement accuracy or thermocouple inertia. A set of equipment, including analog-digital converter EP-90118R, respective software and computer, was used for recording experimental data. Thermocouple readings were registered with the frequency of 10 Hz.

Results of processing the derived thermo-kinetic curves were used to assess the main parameters of thermal cycle of welding: maximum temperature, time of existence of weld pool melt and of weld metal staying in a certain temperature interval, its heating and cooling rate. Structural changes, depending on temperature-rate conditions of weld formation, were studied on welded joint macrosections, using the methods of microprobe analysis, metallography and X-ray diffractometry.

The following characteristics of weld structure were assessed: dendrite spacing λ; dispersion and morphology of γ′-phase, eutectic components of γ-γ′-phases and carbide precipitates; dislocation density and distribution; ROG presence and nature.

Solidification rate **R** and nature of its variation across weld pool front *MO*, according to schematic given in Figure 3, was assessed with 0.2–0.3 mm step with application of the known dependence [17]:

$$\mathbf{R} = v_w \cos \alpha, \quad (1)$$

where **R** is the solidification rate; v_w is the welding speed; α is the angle between the direction of maximum temperature gradient and weld axis (see Figure 4).

Temperature gradient **G** across the solidification front was determined, proceeding from Brody–Flemings relationship:

$$\lambda = A\mathbf{G}^{-m}\mathbf{R}^{-n}, \quad (2)$$

where λ is the value of dendrite spacing, coefficient *A* is proportional to solidification range ΔT, while the exponents at $m = n = 0.32$ express the distance between the axes of dendrites of the first order for HTNA [5, 10]. This relationship at preliminary determination of solidification rate and coefficient *A* allows evaluation of temperature gradient **G** across the solidification front and correlation of temperature-rate conditions and structural perfection of forming weld metal, on the one hand, and process parameters of welding mode, on the other.

Value of coefficient *A* for the studied EBW parameter range was determined by computation-experimental method in keeping with dependence (2). Here, cooling rate **GR** was determined through tangent of the angle of inclination of linear section of thermogram near inflection point T_{L-S}, while dendrite spacing λ was measured on macrosections in the point of thermocouple location.

Microstructure of the metal of welds produced on single crystal samples at complete penetration with fusion surface orientation far from high symmetry {110}, {115} and {111}, is characterized by dendrite form of phase components in all the cases. Presence of both material volumes with inherited orientation of initial single crystal, and of randomly oriented grains is noted (Figure 5). Analysis of parameters of dispersion of weld metal dendritic structure in the range of welding speeds of 12–90 m/h showed that at EBW a high rate of heat removal from solidification front is ensured (Figure 6) and conditions for formation of fine cellular-dendritic structure are created. Minimum values λ = 3–12 μm, depending on the welding mode, are observed in the fusion zone, where maximum temperature gradient is in place. When getting closer to weld axis, value λ increases up to values of 25–55 μm, that corresponds to lowering of cooling rate **GR** (Table 2). A feature of weld metal structure is the presence of a narrow zone at the fusion line (FL), which is characterized by clear inheritance of crystallographic orientation of base metal that is confirmed by the results of X-ray (see Figure 5) and metallographic (Figure 7) studies. This zone is a region of epitaxial growth 0.1–0.5 mm wide without any ROG (see Figure 5, *c*, *d*). Distribution of the intensity of X-ray reflection $I\mathbf{q}_\perp$ is relatively smooth, close to that of the initial metal. Isointensive lines have the form of ellipsoidal curves (see Figure 5, *d*), that corresponds to single-crystal state of metal with uniform distribution of edge dislocations [19–23].

Presence of such a zone with clear inheritance of initial crystallographic orientation points to the possibility of formation of a single-crystal weld under any orientational conditions.

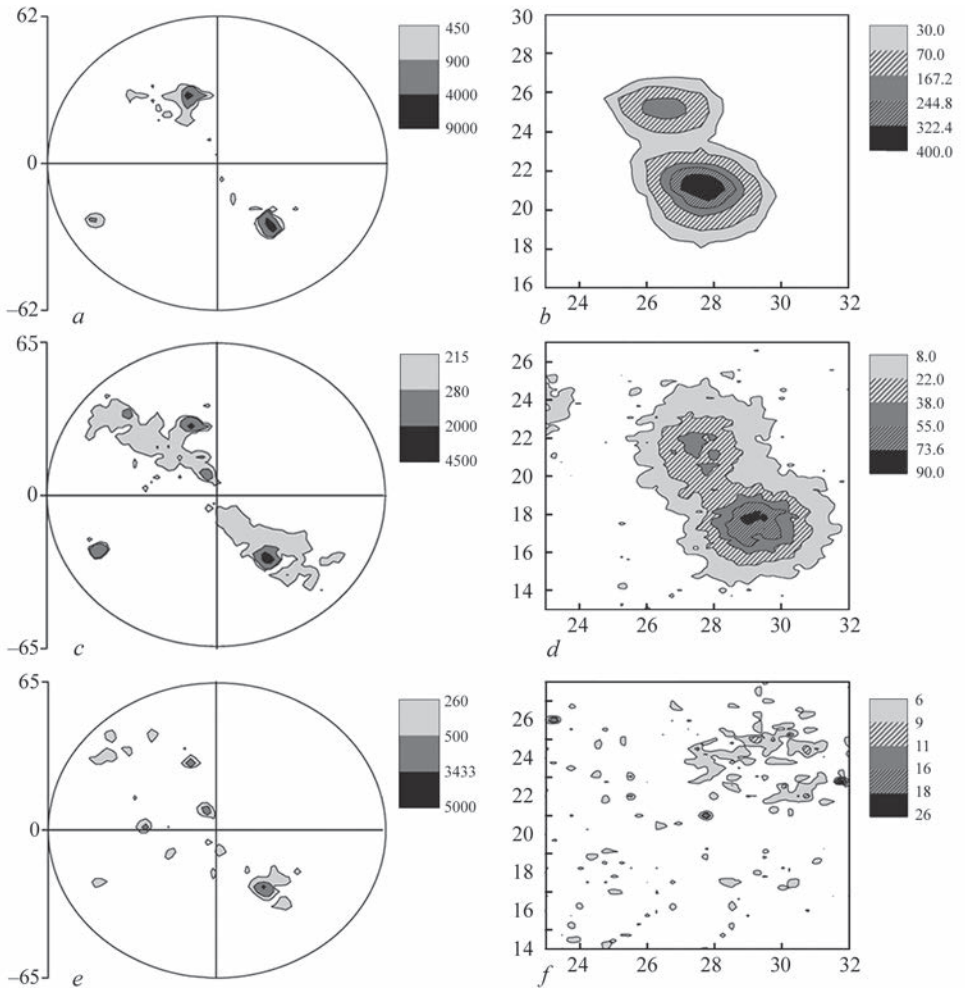

Figure 5. Pole figures {220} and $I\mathbf{q}_{\perp}$ distribution of (022) reflection in different zones of welded joint of asymmetrical crystallographic orientation: *a*, *b* — BM; *c*, *d* — weld at the FL; *e*, *f* — weld axis

Derived experimental results (Figure 8) confirm the known theoretical postulate [17] that thermal conditions across the solidification front change as the dendrites grow from the fusion line towards weld axis. Temperature gradient **G** has maximum values at the FL and decreases towards weld axis, while solidification rate **R** here changes from minimal value at the FL to maximum one at weld axis. Under such thermal conditions of weld metal solidification, a high stability of directional growth of dendrites and maximum refinement of the dendritic structure — up to $\lambda \sim 3$ μm, are ensured in the narrow zone at the FL.

Refinement of structural components of single crystals at optimization of EBW parameters results in a significant reduction of structural and segregational inhomogeneity [10], the main point being improvement of the stability of directional solidification across the front of crystal growth. Analysis of the results of studying the structure and temperature-time and orientational parameters of solidification in different regions of solidification front (Table 3) leads to the conclusion that violation of the perfection of single-crystal structure, that is most often manifested in formation of ROG, occurs in the regions where the value of **G/R** ratio is below the admissible level, which depends on the magnitude of angular deviation

Table 2. Dependence of dendrite structure parameters of JS26 alloy on EBW speed

v_w, m/h	Weld metal λ at FL, μm	Weld metal λ on its axis, μm
90	3.4	33.3
53	3.3	25.0
17	12.5	56.3
Note. BM λ = 200–230 μm.		

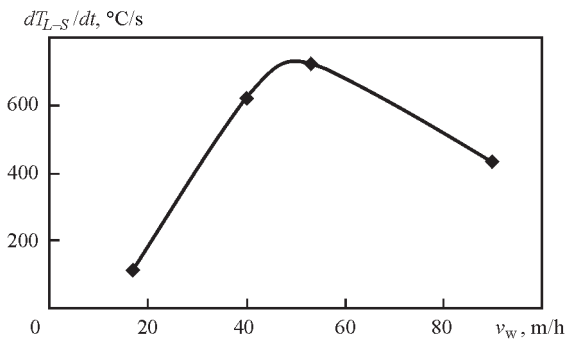

Figure 6. Dependence of cooling rate across solidification front on speed of EBW of JS26 alloy 2.5 mm thick

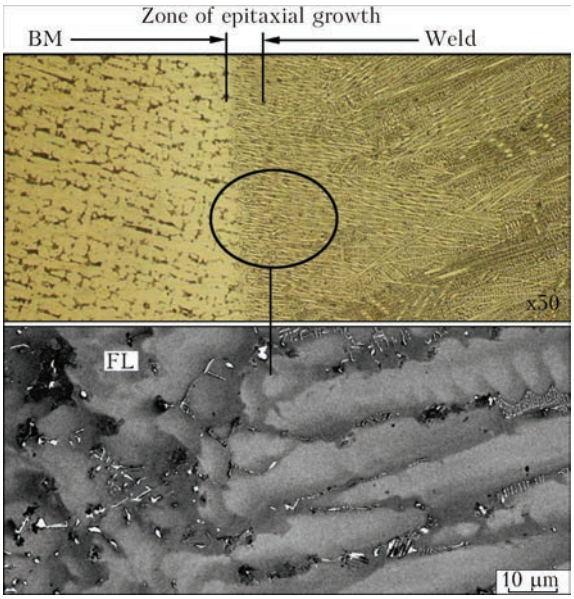

Figure 7. Microstructure of metal of the JS26 joint alloy of asymmetrical crystallographic orientation

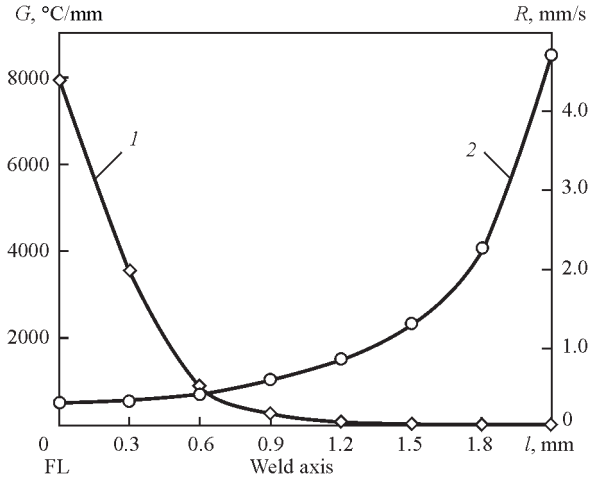

Figure 8. Change of temperature-rate conditions of directional solidification across weld pool solidification front at welding speed of 17 m/h: *1* — value of maximum temperature gradient **G**; *2* — crystallite growth rate **R**

of the direction of maximum temperature gradient from predominant growth orientation <100> across the solidification front (Table 4).

In the considered range of welding modes and thicknesses, 40–50 m/h can be regarded as the optimum speed, at which sound formation of the weld with through-thickness penetration and fusion surfaces close to parallel ones is provided. Some discrepancy with the generally accepted concepts of the influence of welding speed on weld formation and its structure is attributable to the nature of distribution of heat input, which is in place at such penetration between weld pool melt, HAZ and energy removed from penetration channel. When temperature-rate parameters of solidification of the order of **G/R** = 65.10^3 s·°C/mm^2 are reached, the admissible orientation range is expanded considerably, and conditions are in place for directional solidification of weld metal at large angles of deviation $\varphi \geq 45°$ of maximum temperature gradient direction from predominant growth orientation <001> across the pool solidification front.

It is obvious that at such temperature-rate conditions the zone of concentrational overcooling ahead of solidification front is narrowed to the level, at which thermomechanical fluctuations cannot lead to nucleation of new solidification centers [5]. It should be noted that the results shown in Figure 8 and Table 3 are given as an illustration of realization of the proposed procedural approach. In this study, investigations were performed on samples with different crystallographic orientations, welding modes and conditions, the results of which led to certain conclusions. Figures 9 and 10 show one of the results of such an approach. In welding of crystallographically asymmetrical samples (Figure 10, *a*) a weld with perfect single crystal structure was formed (Figures 9

Table 3. Temperature-rate parameters of weld metal solidification across weld pool solidification front at welding speed of 53 m/h obtained by computation-experimental method

Point number	*l*, mm	*R*, mm/s	*G*, °C/mm	*GR*, °C/s	*G*/*R*, s·°C/mm^2
1	FL	1.28	139074	178015	108652
2	FL + 0.3	2.0	48828	97656	24414
3	FL + 0.6	2.6	591	1537	227
4	FL + 0.9	3.3	219	722	66
5	FL + 1.2	3.8	161	612	42
6	FL + 1.5	4.5	97	437	22
7	FL + 1.8 (weld axis)	11.09	29	321	2.6
Note. l — distance from the fusion line.					

Table 4. Admissible deviations φ of the direction of maximum temperature gradient **G** from predominant crystal growth orientation <001> across weld pool solidification front depending on **G/R** value

φ, deg, ≤	0–5	10–15	20	25	30	35	40–45
G/*R*, s·°C/ mm^2	0.2–0.23	1.2–1.5	230	1500	$19 \cdot 10^3$	$25 \cdot 10^3$	$(62–68) \cdot 10^3$

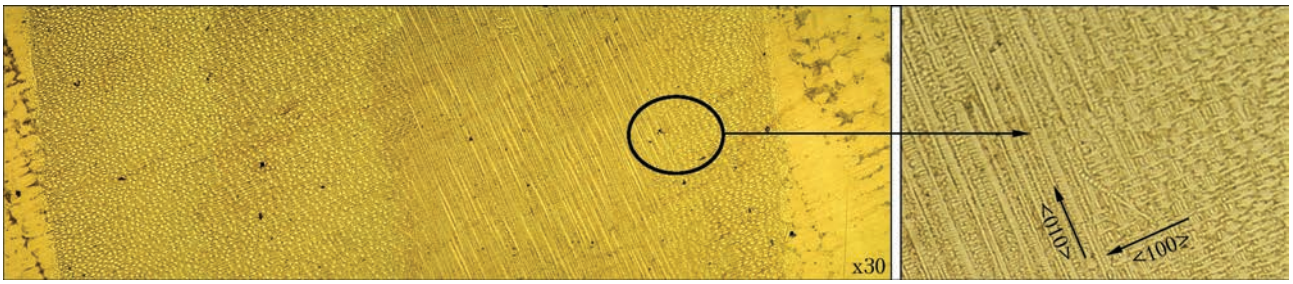

Figure 9. Weld metal microstructure with initial asymmetrical crystallographic orientation of welded joint produced with control of temperature-rate parameters of weld pool solidification

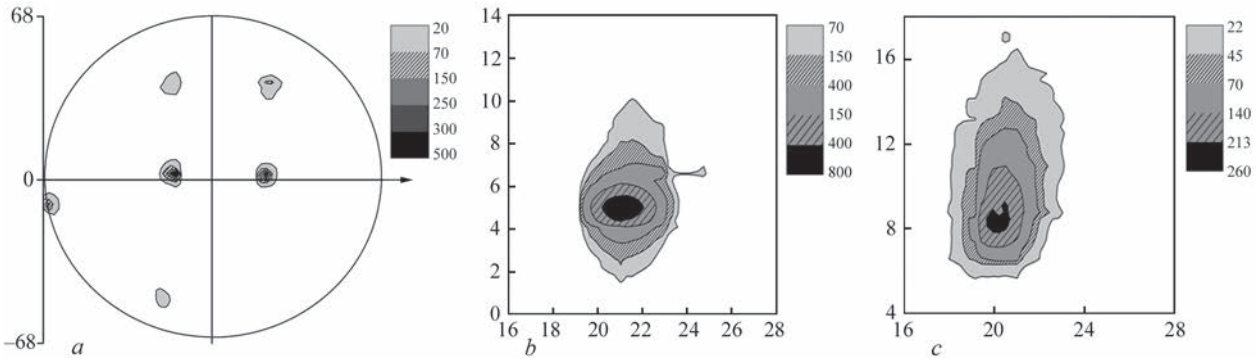

Figure 10. Pole figures {311} of metal being welded (*a*) and $I\mathbf{q}_{\perp}$ distribution of reflection (311) (*b*, *c*) in different zones of welded joint with asymmetrical crystallographic orientation produced with control of temperature-rate parameters of weld pool solidification: *b* — BM; *c* — weld metal (numerical values along the axes are given in degrees)

and 10, *c*). Just a change of crystallographic index of weld metal orientation from <100> to <010> is found in high-gradient zone of epitaxial growth. Here, no grains formed, and, on the whole, a weld with single-crystal structure was produced.

Thus, it is shown that optimization of temperature-rate parameters of solidification of weld pool metal through selection of welding modes enables producing welded joints with perfect single-crystal structure at a large ($\varphi \sim 45°$) deviation of the direction of maximum temperature gradient from predominant growth orientation <100>. Such an approach will allow development and introduction into production of a technology of welding and repair of single-crystal items of a complex shape.

Conclusions

1. A computational-experimental procedure is proposed for evaluation of temperature-rate parameters of solidification across the front of weld pool solidification in EBW.

2. The range of temperature-rate parameters of the process of solidification of weld pool of JS26 alloy was determined, in which a high perfection of single-crystal structure of weld metal and absence of randomly oriented grains are ensured. So, at deviation of maximum temperature gradient direction from predominant growth orientation <100> of the order of $\varphi = 5°$, directional solidification of weld metal is preserved at $\mathbf{G/R} \geq 0.20–0.23$ s·°C/mm, and at $\varphi \sim 45°$ — $\mathbf{G/R} \geq (62–68)\cdot 10^3$ s·°C/mm.

3. Shown is the possibility of controlling formation of weld metal structure in EBW of single crystals of high-temperature nickel alloys through optimization of temperature-rate parameters of the process of weld pool metal solidification, that allows producing joints with perfect single-crystal structure in weldments with crystallographically asymmetrical structure of the joint.

1. (1995) *Superalloys II: Heat-resistant materials for aerospace systems and industrial power plants*. Book 1. Moscow: Metallurgiya.
2. Erickson, G.L., Harris, K. (1994) DS and SX superalloys for industrial gas turbines. In: *Proc. of Conf. on Materials for Advanced Power Engineering* (Belgium, 3–6 Oct. 1994), Pt 2, 1055–1074. Kluwer Acad. Publ.
3. Erickson, G.L. (1995) A new third generation single crystal, casting superalloy. *J. of Metals*, 47(**4**), 36–39.
4. (2006) *Cast heat-resistant alloys. S.T. Kishkin effect*: Sci.-techn. coll. Moscow: Nauka.
5. Shalin, R.E., Svetlov, I.L., Kachanov, E.B. et al. (1997) *Single crystals of nickel heat-resistant alloys*. Moscow: Mashinostroenie.
6. Stroganov, G.B., Chepkin, V.M. (2000) *Cast heat-resistant alloys for gas turbines*, 63–65. Moscow: ONTI MATI.
7. Shah, D.M., Duhl, D.N. (1984) Effect of orientation, temperature and gamma prime size on the yield strength of a single crystal nickel base superalloy. In: *Superalloys*, 105–114. Metallur. Soc. of AIME.
8. Kishkin, S.T., Stroganov, G.B., Logunov, A.V. (2001) *Nickel-based cast heat-resistant alloys*. Moscow: MISIS.

9. Dong, H.B., Yang, X.L., Lee, P.D. (2004) Simulation of equiaxed growth ahead of an advancing columnar front in directionally solidified Ni-base superalloys. *J. Materials Sci.*, **39**, 7207–7212.
10. Kablov, E.N. (2001) *Cast blades of gas-turbine engines (alloys, technology, coatings)*. Moscow: MISIS.
11. Yushchenko, K.A., Gakh, I.S., Zadery, B.A. et al. (2013) Influence of weld pool geometry on structure of metal of welds on high-temperature nickel alloy single crystals. *The Paton Welding J.*, **5**, 45–50.
12. Yushchenko, K.A., Zadery, B.A., Gakh, I.S. et al. (2013) On nature of grains of random orientation in welds of single crystals of heat-resistant nickel alloys. *Metallofizika i Nov. Tekhnologii*, 35(**10**), 1347–1357.
13. Yushchenko, K.A., Zadery, B.A., Zvyagintseva, A.V. et al. (2008) Sensitivity to cracking and structural changes in EBW of single crystals of heat-resistant nickel alloys. *The Paton Welding J.*, **2**, 6–13.
14. Gakh, I.S. (2011) *Physical-technological peculiarities of electron beam welding of high-nickel heat-resistant alloys with single-crystal structure*: Syn. of Thesis for Cand. of Techn. Sci. Degree. Kiev: PWI.
15. Rabkin, D.M., Ignatiev, V.G., Dovbishchenko, I.V. (1982) *Arc welding of aluminium and its alloys*. Moscow: Mashinostroenie.
16. Rykalin, N.N. (1951) *Calculations of thermal processes in welding*. Moscow: Mashgiz.
17. Frolov, V.V., Vinokurov, V.A., Volchenko, V.N. et al. (1988) *Theoretical principles of welding*. Moscow: Vysshaya Shkola.
18. Solomatova, E.S., Trushnikov, D.N., Belenky, V.Ya. et al. (2014) Evaluation of temperature in vapor gas channel in EBW of dissimilar metals. *Sovr. Problemy Nauki i Obrazov.*, **2**, 21–26.
19. Panin, V.E., Likhachev, V.A., Grinyaev, Yu.V. (1985) *Structural levels of deformation of solids*. Novosibirsk: Nauka.
20. Likhachev, V.A., Panin, V.E., Zasimchuk, E.E. et al. (1989) *Cooperative deformation processes and localization of deformations*. Kiev: Naukova Dumka.
21. Malygin, G.A. (1995) Self-organizing of dislocations and localization of slipping in plastically deformed crystals. *Fizika Tv. Tela*, 37(Issue 1), 3–42.
22. Sarafanov, G.F. (1998) To theory of formation of heterogeneous dislocation structures. *Fizika Metallov i Metallovedenie*, 85(Issue 3), 46–53.
23. Koneva, N.A., Kozlov, E.V. (1990) Physical nature of staging of plastic deformation. *Izvestiya Vuzov, Fizika*, **2**, 89–106.

Received 17.05.2016